REGULAR ARTICLE

CrossMark

Solubilized eggshell membrane supplies a type III collagen-rich elastic dermal papilla

Eri Ohto-Fujita[1] · Miho Shimizu[1] · Shoei Sano[1] · Masashi Kurimoto[1] · Kai Yamazawa[1] ·
Tomoaki Atomi[2] · Takashi Sakurai[3,4] · Yoshihiko Murakami[5] · Taku Takami[5] ·
Tomoaki Murakami[6] · Kotaro Yoshimura[7] · Yukio Hasebe[8] · Yoriko Atomi[1]

Abstract

Signs of aging in facial skin correlate with lifespan and chronic disease; however, the health of aging skin has not been extensively studied. In healthy young skin, the dermis forms a type III collagen-rich dermal papilla, where capillary vessels supply oxygen and nutrients to basal epidermal cells. Chicken eggshell membranes (ESMs) have been used as traditional medicines to promote skin wound healing in Asian countries for many years. Previously, we designed an experimental system in which human dermal fibroblasts (HDFs) were cultured on a dish with a solubilized ESM (S-ESM) bound to an artificial phosphorylcholine polymer; we found that genes that promoted the health of the papillary dermis, such as those encoding type III collagen, were induced in the S-ESM environment. The present study found that a gel with a ratio of 20% type III/80% type I collagen, similar to that of the baby skin, resulted in a higher elasticity than 100% type I collagen ($p < 0.05$) and that HDFs in the gel showed high mitochondrial activity. Thus, we decided to perform further evaluations to identify the effects of S-ESM on gene expression in the skin of hairless mice and found a significant increase of type III collagen in S-ESM. Picrosirius Red staining showed that type III collagen significantly increased in the papillary dermis after S-ESM treatment. Moreover, S-ESM application significantly improved human arm elasticity and reduced facial wrinkles. ESMs may have applications in extending lifespan by reducing the loss of tissue elasticity through the increase of type III collagen.

Keywords Extracellular matrix · Eggshell membrane · Papillary dermis · Geroscience · Type III collagen

---

Eri Ohto-Fujita, Miho Shimizu and Yoriko Atomi contributed equally to this work.

✉ Yoriko Atomi
yatomi@cc.tuat.ac.jp

[1] Material Health Science Laboratory, Graduate School of Engineering, Tokyo University of Agriculture and Technology, 2-24-16 Nakacho, Koganei-shi, Tokyo 184-8588, Japan

[2] Faculty of Health Sciences, Department of Physical Therapy, Kyorin University, 5-4-1 Shimorenjaku, Mitaka-shi, Tokyo 181-8612, Japan

[3] Department of Life Sciences, The Graduate School of Arts and Sciences, The University of Tokyo, 3-8-1, Komaba, Meguro-ku, Tokyo 153-8902, Japan

[4] Present address: Astellas Institute for Regenerative Medicine, 33 Locke Drive, Marlborough, MA 01752, USA

[5] Department of Organic and Polymer Materials Chemistry, Faculty of Engineering, Tokyo University of Agriculture and Technology, 2-24-16 Nakacho, Koganei-shi, Tokyo 184-8588, Japan

[6] Laboratory of Veterinary Toxicology, Cooperative Department of Veterinary Medicine, Tokyo University of Agriculture and Technology, 3-5-8 Saiwai-cho, Fuchu-shi, Tokyo 183-8509, Japan

[7] Department of Plastic Surgery, Jichi Medical University, 3311-1 Yakushiji, Shimotsuke-shi, Tochigi-ken 329-0498, Japan

[8] Almado Inc., 3-6-18 Kyobashi, Chuo-ku, Tokyo 104-0031, Japan

Introduction

The skin is the outermost tissue and is useful for monitoring signs of aging and health. Facial appearance reflects longevity (Gunn et al. 2013) and heart block (Roshdy et al. 2018). Skin wrinkles (Vierkotter et al. 2015) and elasticity (Çildağ and Çildağ 2017) are also correlated with lung fibrosis. Therefore, additional studies of the mechanical properties of the extracellular matrix are needed.

The skin consists of the epidermis, basement membrane, as the epidermis–dermal interface dermis and subcutaneous tissue. The dermis has two distinct layers, the superficial papillary dermis and the underlying reticular dermis. In young healthy skin, the dermis forms the papillary layer, which pushes up the epidermis. In the papillary layer, the cellular environment is composed of capillary vessels, which supply oxygen and nutrients to the basal epidermal cells (Archid et al. 2012; Auer et al. 1994; Braverman 1983; Konttinen et al. 2003; Sauermann et al. 2002; Wang 2005; Wang et al. 2003), type III collagen (Meigel et al. 1977) and decorin (Schonherr et al. 1993). The mechanical function of type III collagen has not been fully elucidated; however, ruptured blood vessels and wounded skin have been reported in Col3a1$^{-/-}$ mice (Liu et al. 1997), whereas dermal and blood vessel collagen fibrillogenesis was affected in Col3a1 mutant mice (D'Hondt et al. 2018). Thus, type III collagen is essential for tissue integrity and homeostasis, including that of the skin.

In aged skin, dermal collagen synthesis and cell populations decrease and matrix metalloproteinase (MMP) levels increase (Chung et al. 2001; Varani et al. 2000). Additionally, dermal thickness decreases with the loss of dermal collagen content (Castelo-Branco et al. 1994; Kurban and Bhawan 1990). Moreover, as the capillaries decrease, nutrient supply from capillaries to the epidermis becomes difficult (Vybohova et al. 2012). When the skin becomes thinner, the influence of ultraviolet rays on the cells becomes stronger, resulting in DNA damage and apoptosis (Gilhar et al. 2004). This can cause a vicious cycle of increased skin damage; thus, prevention of skin aging and damage is urgently needed.

In China and Japan, chicken eggshell membranes (ESMs) have been used as wound dressings for more than 400 years. ESM mainly consists of collagen types X, V and I, cysteine-rich proteins (Arias et al. 1991; Wong et al. 1984), proteoglycans (Arias et al. 1992; Du et al. 2015; Ha et al. 2007) and hyaluronic acid (Liu et al. 2014). We investigated the effects of ESMs on cells in our previous study and showed that moderate amounts of solubilized ESMs (S-ESMs) retained the cells in a healthy state (Ohto-Fujita et al. 2011). Moreover, human dermal fibroblasts (HDFs) adhered to a dish with S-ESM bound to a particular environment. As a result, in the same cellular environment as the dermis, the expression of genes encoding type III collagen, decorin and MMP2, which promote young skin (papillary layer), was induced. However,

the effects of S-ESM on skin aging in animal models have not been studied.

Therefore, in this study, we first examine the anti-aging effects of type III collagen using collagen gel and human fibroblast cell in vitro and then chicken S-ESM in the dermal papilla using animal and human models to provide a comprehensive understanding of the applications of this material.

Methods

Cell culture in 2D collagen gel analysis

HDFs derived from infant skin were isolated as described previously (Aiba-Kojima et al. 2007) and were cultured with Dulbecco's modified Eagle's medium (Wako Pure Chemical Industries) containing 10% fetal bovine serum (Sigma-Aldrich) and a penicillin–streptomycin–neomycin antibiotic mixture (1×; Gibco). HDFs were used at passage numbers 5–9. For analysis of collagen gel elasticity, type I collagen was prepared in-house from rat tails based on a previously reported method (Yamato et al. 1992) and type III collagen from bovine skin was purchased from Nippi (PSC-3-100-100; Tokyo, Japan). The 2D collagen gel (0.3%) was prepared by mixing type I and III collagen solutions (5.0 mg/mL), 10× medium and reconstruction buffer (0.02 M HEPES, 0.03 M NaHCO$_3$, 0.05 M NaOH). The ratios of type III collagen to total collagen were 0%, 10%, 20%, 40%, 60% and 80%. HDFs were cultured on 2D collagen gels.

Mechanical properties of collagen gels

Final 0.4% collagen gels were prepared using a method similar to that described above and elasticity was measured with a rheometer (RS600; Thermo Electron, Germany). Hydrogel properties, including the storage modulus (G') and loss modulus (G''), were evaluated using a rheometer (RS600; Thermo Electron; sensor: PP35Ti). All measurements were performed at a shear stress of 0.5 Pa, with a frequency of 1.0 Hz and G' was plotted for each collagen gel with different type III/I ratios.

Analysis of protein expression in cells cultured on collagen gels

HDFs were cultured on collagen gels. After culturing for 24 h, cells were fixed using a formalin solution and immunostained with rabbit anti-human collagen III, N-terminal antibodies (Sigma-Aldrich; SAB4500367). Goat anti-rabbit IgG H&L (Alexa Fluor 555; ab150082; Abcam, Cambridge, UK) was used as the secondary antibody. For protein expression analysis, fluorescent images were obtained with a confocal laser microscope and the fluorescence intensity per cell was semi-quantified ($n = 15$). Relative intensities were normalized and plotted.

Measurement of mitochondrial activity

HDFs were cultured on hetero collagen gels with a type I:type III collagen ratio of 10:0 or 8:2. The cells were stained with 3 μg/mL JC-1 (Molecular Probes, Eugene, OR, USA) for 1 h at 37 °C. JC-1 fluorescence was observed with a confocal laser scanning microscope and the red fluorescence (590 nm)/green fluorescence (527 nm) intensity was obtained from a 1-mm^2 area of three observed fields (about 17,400 cells). Relative intensities were plotted.

Microscopy

Tissue sections and stained cell images were observed with a Nikon A1RMP microscope and fluorescence intensities were semi-quantified using Nikon NIS-elements software.

Animals

Animal experiments were conducted with the ethical approval of the University of Tokyo Animal Experiments Committee and Tokyo University of Agriculture and Technology Animal Experiments Committee.

Topical S-ESM application in mice

Specific pathogen-free hairless mice (Hos: HR-1, 6 weeks of age, male) were purchased from Hoshino Laboratory Animals, Inc. (Ibaraki, Japan). Mice were divided into two experimental groups ($n = 9$ each) and were treated with 0% S-ESM (control) or 10% (w/v) S-ESM in vehicle (7% butylene glycol, 1% pentylene glycol, 4% glycerin, 0.2% phenoxyethanol aqueous solution). S-ESM was provided by Almado Inc. (Tokyo, Japan). The test solution (40 μL) was applied twice a day to the back skin for 10 days. Skin biopsy samples from each mouse were obtained with a biopsy punch (φ4 mm), washed in phosphate-buffered saline and stored in RNAlater solution (Life Technologies). For the evaluation of each layer, biopsy skin samples were sectioned with a vibratome (Leica VT1200s) into 100-μm-thick sections.

Paraffin-embedded skin sections and type III collagen staining

Paraffin sections of hairless mouse skin after S-ESM application were prepared and stained with Picrosirius Red (Polysciences, Inc.). Control ($n = 5$) and 10% S-ESM-treated sections ($n = 5$) were stained. Images of the stained samples were acquired with a polarizing microscope (Olympus BX53) and then the green area (type III collagen)/red area (type I collagen) was quantified using Image J.

RNA extraction and quantitative real-time PCR

Skin samples were crushed using a frozen cell crusher (Cryo-Press, Microtech, Co., Ltd.). From the crushed tissue, total RNA was isolated with TRIzol Reagent (Life Technologies, USA) and purified with Maxwell® 16 Tissue and Cell Total RNA LEV Systems (Promega Co., USA) according to the supplier's protocol. Total RNA was quantified by spectrophotometry and aliquots of total RNA (200 ng) were applied for cDNA synthesis using a Takara Prime Script RT reagent kit (Perfect Real Time). cDNA synthesis conditions were as follows: 15 min at 37 °C and 15 s at 85 °C. One microliter of cDNA was used for real-time PCR. SYBR Premix Ex TaqTM II (Takara) was used for gene amplification on a Thermal Cycler Dice Real-Time System (Takara). Primers were designed by Sigma-Genosys (Hokkaido, Japan). The sequences are listed in Table 1. Triplicate reactions were performed for each sample. GAPDH was used as an internal control.

Table 1 Primer sequence (5′-3′)

Gene	Forward primer	Reverse primer
Gapdh	AGCTTGTCATCAACGGGAAG	TTTGATGTTAGTGGGGTCTCG
Col1a1	CATGTTCAGCTTTGTGGACCT	GCAGCTGACTTCAAGGGATGT
Col3a1	TCCCCTGAGAATCTGTGAATC	TGAGTCGAATTGGGGATGT
Col4a1	TTAAAGGACTCCAGGGACCAC	CCCACTGAGCCTGTAACAC
Mmp2	GGAGAAGGCTGTGTTCTTCG	AGGCTGGTCAGTGGCTTG
Mmp3	TTGTTCTTTGATGCAGTCAGC	GATTTGCGCCAAAAGTGC
Decorin	GAGGAGAAGTGAGGGGAGCA	GATTATCTCATGTATTTTTCACGACCTT
Elastin	TGGAGCAGGACTTGGAGGT	CCTCCAGCACCATACTTAGCA
Has2	GGCGGAGGACGAAGTCTATG	ACACATAGAAACCTCTCACAATGC
Hsp47	GCGGACTGCCTGGTAAAC	GAAGGAGGAGCGCATGG
Tgf-β1	GGATACCAACTATTGCTTCAGCTC	GTGTCCAGGCTCCAAATATAGGG
Tgf-β3	CGGATGAGCACATAGCCAAGC	CCAGACCCAAGTTGGACTCTCT

Participants for the human study of the effects of topical S-ESM on skin elasticity

Approval for this study was obtained from the Ethics Committee of the University of Tokyo. All volunteers were included in the study after providing written informed consent. Fourteen healthy volunteers (all women; age 22–54 years [mean 37.1 ± 12.6 years]) participated in this study. These 14 individuals were randomly divided into the S-ESM group ($n = 7$; mean age 36.7 ± 4.8 years) and the control group ($n = 7$; mean age 37.4 ± 5.1 years) and then underwent 12 weeks of supervised application of 1% or 0% S-ESM in vehicle to arm skin. The participants were advised to avoid applying topical drugs or moisturizers on the tested zones during the experiment. The volunteers were acclimated for 15 min in a conditioned room (22 ± 2 °C, $50\% \pm 10\%$ relative humidity) before the experiment.

Study protocol for analysis of the effects of topical S-ESM on skin elasticity

This was a double-blind, placebo-controlled study. S-ESM was provided by Almado Inc. (Tokyo, Japan). Moisturizing lotion either with 1% S-ESM as a test ingredient or without S-ESM (control) was used. The vehicle was an aqueous solution of 1,3-butylene glycol, glycerol and 1,2-hexanediol. Other minor components of the moisturizer were as follows: PEG-75, lysolecithin, α-glucan oligosaccharide, rose extract, hydrolyzed collagen, sorbitol, phenoxyethanol, *Saccharomyces cerevisiae* extract, fucoid extract, aloe extract, *Panax ginseng* extract, *Scutellaria* root extract, arnica extract, cucumber fruit extract, common English ivy extract, European elder extract, Malva extract, stinging nettle extract and dipropyleneglycol. A moisturizing cream containing 1% S-ESM as a test ingredient or no S-ESM (control) was also used. The base was an aqueous solution of 1,3-butylene glycol and glycerol. Minor components of the cream were as follows: squalene, dimer dilinoleic acid, stearic hydrogenated castor oil, 1,2-hexanediol, hydroxyethyl acrylate/acryloyldimethyl taurine, Polysorbate 60, sorbitan isostearate, xanthan gum, platinum, α-glucan oligosaccharide, hydrolyzed collagen, hyaluronate sodium, phenoxyethanol, rose extract and polysorbate80. Moisturizing lotion and cream were both applied in the morning and evening. The control group consisted of the base formulation without S-ESM. Participants were instructed to avoid using any other product or detergent during the test trial. The test products were applied to the forearm and upper arm skin for 12 weeks twice daily.

Biophysical measurements for analysis of the effects of topical S-ESM on skin elasticity

Skin elasticity was determined using a Cutometer MPA 580 (Courage+Khazaka, Cologne, Germany). Visco-elastic properties were measured according to the manufacturer's instructions with the following parameters: 300 mbar; on-time, 3 s; off-time, 3 s; R5 = Ur/Ue (net elasticity of the skin without viscous deformation); and R7 = Ur/Uf (biological elasticity) (Krueger et al. 2011). Elasticity was determined by a Cutometer using mode 1, in which measurements were performed with constant negative pressure. The average values of three measurements were used in subsequent calculations.

We measured the following four regions: inner and outer sides of the forearm (midway between the wrist and elbow) and inner and outer sides of the upper arm (midway between the acromion and olecranon), with randomization of the left and right sides. To measure the same regions of the participant, we constructed an arm chamber and recorded the region of interest for each participant; thus, the same region was measured every time. The volunteers were acclimated for 15 min in a conditioned room (22 ± 2 °C, $50\% \pm 10\%$ relative humidity) before the experiment.

Study design for analysis of wrinkles in women

The effects of S-ESM on skin wrinkles were evaluated in a randomized, double-blind, controlled trial. Measurement of crow's feet wrinkles was performed at the beginning of the study and after 2 weeks of treatment. The study was approved by the Ethical Committee of Tokyo University of Agriculture and Technology, Tokyo, Japan and all participants provided informed consent for participation. Before conducting each measurement, the face of the participant was washed and she was allowed to sit and rest for 15 min in a room with a controlled environment at 25 ± 1 °C with a relative humidity of $60\% \pm 5\%$. Participant satisfaction and adverse reactions experienced using the lotion were assessed at the end of the study.

Participants for analysis of wrinkles in women

For the double-blind comparative study on the effects of S-ESM on skin wrinkles, 30 healthy women who appeared to have well-defined crow's feet wrinkles were recruited. Primary exclusion criteria were as follows: being pregnant or breastfeeding, having a history of allergic or cosmetic medicine, or taking hormone replacement therapy. Furthermore, volunteers who had abnormalities of the skin appearing after patch tests with the test lotion or replica reagent were also excluded from the study. For analysis of the effects of S-ESM on face wrinkles, 21 volunteers (mean age 43.9 ± 8.6 years, range 30–56 years) were included in the study after

prescreening. The main component of the test sample was 2% S-ESM in aqueous BG. Minor components were as follows: sodium hyaluronate, rose extract, *Glycyrrhiza* extract and squalene. Components of the control lotion were as follows: water, BG, sodium hyaluronate, rose extract, *Glycyrrhiza* extract and squalene. The test sample was applied to the corner of the eyes and the control sample was applied to the other side three times daily for 2 weeks. For each application, 0.12 g (three drops) was applied to each side. For each participant, assignment managers randomly assigned test samples for the left and right side of the face.

Measurement parameters for analysis of wrinkles in women

Researchers performed a blinded evaluation of skin wrinkles before and after the 2-week treatment. Two-dimensional images were evaluated with replicas using oblique lighting (wrinkle area ratio). Dermatologists evaluated the wrinkle grade of participants following the Eight-grade Wrinkle Scoring scale (grade 0 to 7) issued by the Japan Cosmetic Industry Association (Task Force Committee for Evaluation of Anti-Aging Function 2007) and values from 1 (a few indistinct, shallow wrinkles observable) to 5 (deeper wrinkles observable) were assigned.

Evaluation regions were at the right or left corner of the eye. Skin replicas were collected on the 20 mm × 20 mm area at 5 mm from the lateral angle of the eye, using a silicon-based replica regent (SILFLO; FLXICO Developments Ltd.). The replica images were taken using a super-high pixel digital camera (EOS 6D; Canon) aligned perpendicularly. In the replica, the lines derived from wrinkles on the face surface formed convex structures and application of projecting light provided reproducible shadows according to the shape of the wrinkles. The shadow region in a 10 mm × 10 mm (324 × 324 pixels) area confirmed in both replicas from the pre-test (0 weeks) and those after 2 weeks of treatment near the outer corner of the eyes was considered a landmark and was defined as the wrinkle area (evaluated as the area ratio [%]).

Before quantifying the area of replica shadows, binarization processing was performed using ImageJ image analysis software. The threshold setting at the time of binarization processing was set to detect the shape of the shadow, which was made constant between the 0- and 2-week replicas in order to compare change in wrinkles. Using ImageJ, circular shadows with an aspect ratio of 1 were excluded as being irrelevant to wrinkles. Mean values, standard deviations and standard errors were calculated for the area ratios of the S-ESM application area to the S-ESM-free vehicle application area and Student's *t* tests were used to calculate the significance of the difference. Questionnaires were given to the participants to evaluate difficulties during use, usage conditions and effectiveness.

Statistical analysis

The mean values and standard errors (SEs) were calculated. Student's *t* tests for paired data were used to compare the mean values of the mechanical parameters before and after application of the test cosmetics. Differences with *P* values of less than 0.05 were considered statistically significant.

Results

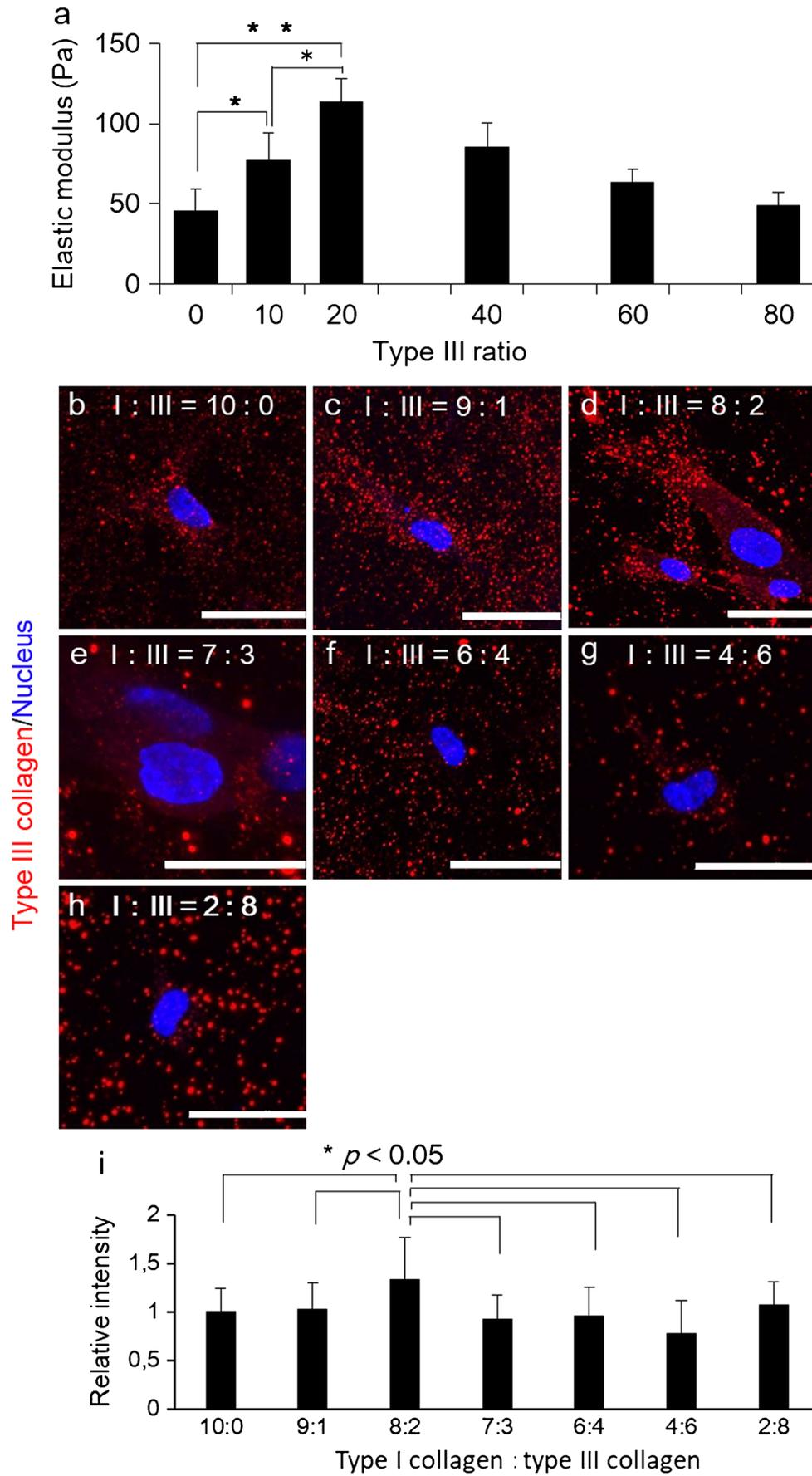### ESM acted as a natural wound-healing material

Chicken ESM has been used as a wound healing dressing in China and Japan and in Sumo wrestlers as a wound healing material in Japan; however, the effects of ESM on cells and tissues have not been clarified. Accordingly, in this study, we explored the effects of ESM on wound skin using full-thickness wounds made on the dorsal skin of slow-healing diabetic mice. Our results showed that ESM tended to produce homogeneous healing tissue and promote thinner layers of type III collagen expression at the early phase of wound healing (Fig. S1).

Type III collagen synthesized by HDFs and the high modulus of elasticity in gels with collagen ratios similar to those of young skin

There are 28 collagens expressed in humans (Exposito et al. 2010); type I and III collagens are the major fibril-forming collagens in the skin. To investigate the relationships between type III collagen content in the dermis and skin elasticity, we prepared collagen gels with a different ratio of type I collagen:type III collagen and measured the elastic modulus. The results revealed that the elasticity was highest in the gel with a type III to type I ratio of 20:80 (Fig. 1a). This ratio was the same as that of young skin. Interestingly, immunostaining of the gels with anti-type III collagen antibodies (Fig. 1b–i) showed that type III collagen protein synthesis was also high at this ratio (Fig. 1d). These results showed that a young skin environment was optimal for dermal fibroblasts to synthesize type III collagen.

The mitochondrial activity of fibroblasts was significantly higher when grown on 20% type III collagen

For evaluation of cell physiology, JC-1 was used to investigate the effects of 20% type III collagen gels on mitochondrial activity. JC-1 accumulates in the mitochondrial membrane in a voltage-dependent manner and can be used to monitor mitochondria activity. In normal polarizing mitochondria, JC-1 aggregates within mitochondria and a fluorescence

wavelength shift from green at 527 nm to red at 590 nm occurs after excitation at 490 nm (Cossarizza et al. 1994; Dorrie et al. 2001). In contrast, monomeric JC-1 present in cells with a depolarized mitochondrial membrane emits only green fluorescence at 527 nm. Thus, dermal fibroblasts cultured on gels with various collagen ratios were stained with JC-1 and observed under a microscope (Fig. 2a–d) and the ratio of JC-1 aggregates (red fluorescence)/JC-1 depolarization (green fluorescence) was plotted to determine mitochondrial activity (Fig. 2e). These results showed that the mitochondrial activity of fibroblasts was significantly higher on gels with 20% type III collagen, the proportion observed in the fetal skin (Fig. 2c, d, e), than the control type I collagen gel (Fig. 2a, b, e).

S-ESM application for 10 days upregulated type III collagen, MMP2 and decorin in the skin of hairless mice by altering the type III/I collagen ratio

To confirm the responses of HDFs, we analyzed changes in gene expression in the dorsal skin of hairless mice after application of S-ESM (Fig. 3a–i). The results showed that extracellular matrix (ECM) molecules, such as type III collagen (Fig. 3b), decorin (Fig. 3g), MMP2 (Fig. 3e) and hyaluronan synthase 2 (Fig. 3i), were upregulated significantly following application of 10% S-ESM solution compared with those in the 0% S-ESM control. The levels of type I collagen (Fig. 3a), elastin (Fig. 3d) and MMP3 (Fig. 3f) were also upregulated; however, the differences were not significant. Heat shock protein 47 (Fig. 3h) and type IV (Fig. 3c) collagen were not upregulated. These results suggested that topical S-ESM application may induce upregulation of gene expression associated with synthesis and degradation of the ECM in dermal tissue.

S-ESM application increased type III collagen in the papillary dermis

Next, we analyzed gene expression in skin sections from mice (Fig. 4a). Significant increases in the expression of genes encoding type III collagen, decorin and MMP2 were confirmed in L2–L4 of the papillary dermis (Fig. 4b; Fig. S2). Picrosirius Red staining of skin sections after S-ESM application showed significant increases in type III collagen fibers (Fig. 4c–m; Fig. S3).
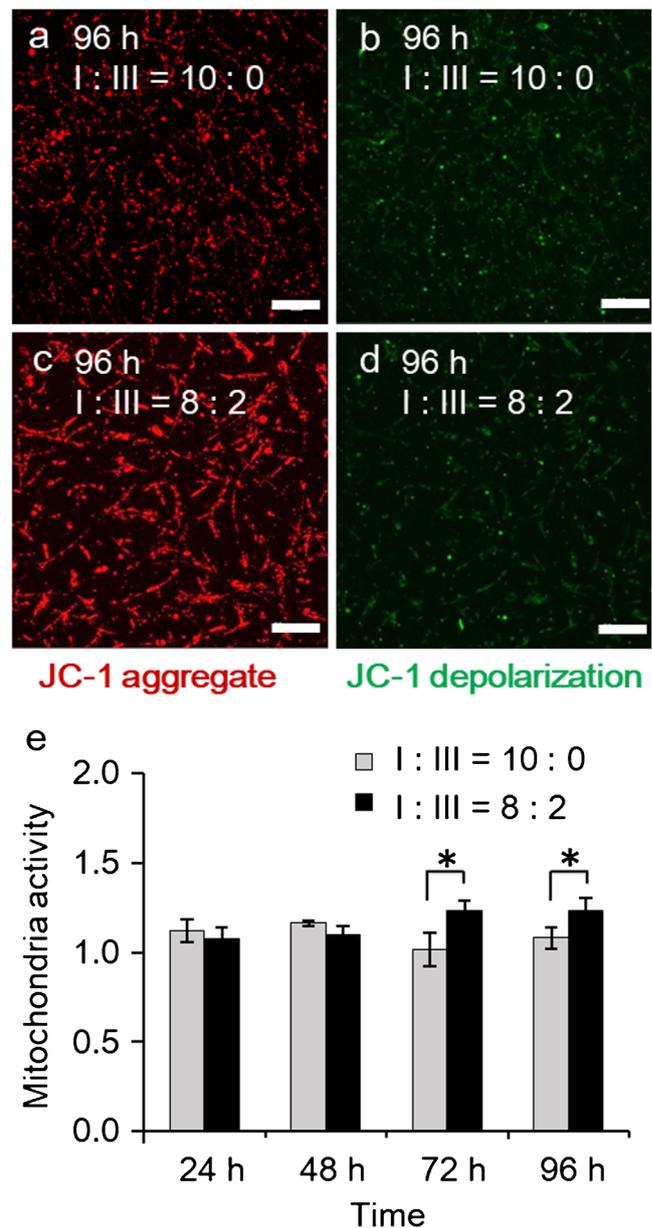

Fig. 2 The mitochondrial activity of fibroblasts was significantly higher on collagen gels containing 20% type III collagen. **a–d** Gels with type I:III collagen ratios of 10:0 or 8:2 were prepared and human dermal fibroblasts were cultured on the gels for 96 h. One hour after addition of JC-1, the fluorescence was observed with a confocal laser scanning microscope. Bar = 200 μm. **e** The ratio of JC-1 aggregate (red fluorescence)/JC-1 depolarization (green fluorescence) was graphed as the mitochondrial activity. I:III indicates type I collagen to type III collagen ratio

Effects of S ESM on the elasticity of arm skin in women

We surprisingly found that the genes encoding type III collagen, decorin and MMP2, which form an environment similar to that of young papillary dermal skin, were induced both in an in vitro system in which S-ESM was covalently attached to an

Fig. 3 Increased ECM-related gene expressions in the skin of hairless mice after S-ESM solution application for 10 days. ECM-related gene expression in the skin after application of 0% or 10% S-ESM to the back skin of hairless mice for 10 days. Means ± SDs are presented ($n = 9$). *$p <$ 0.05 (nonpaired sample t tests, two-tailed tests)
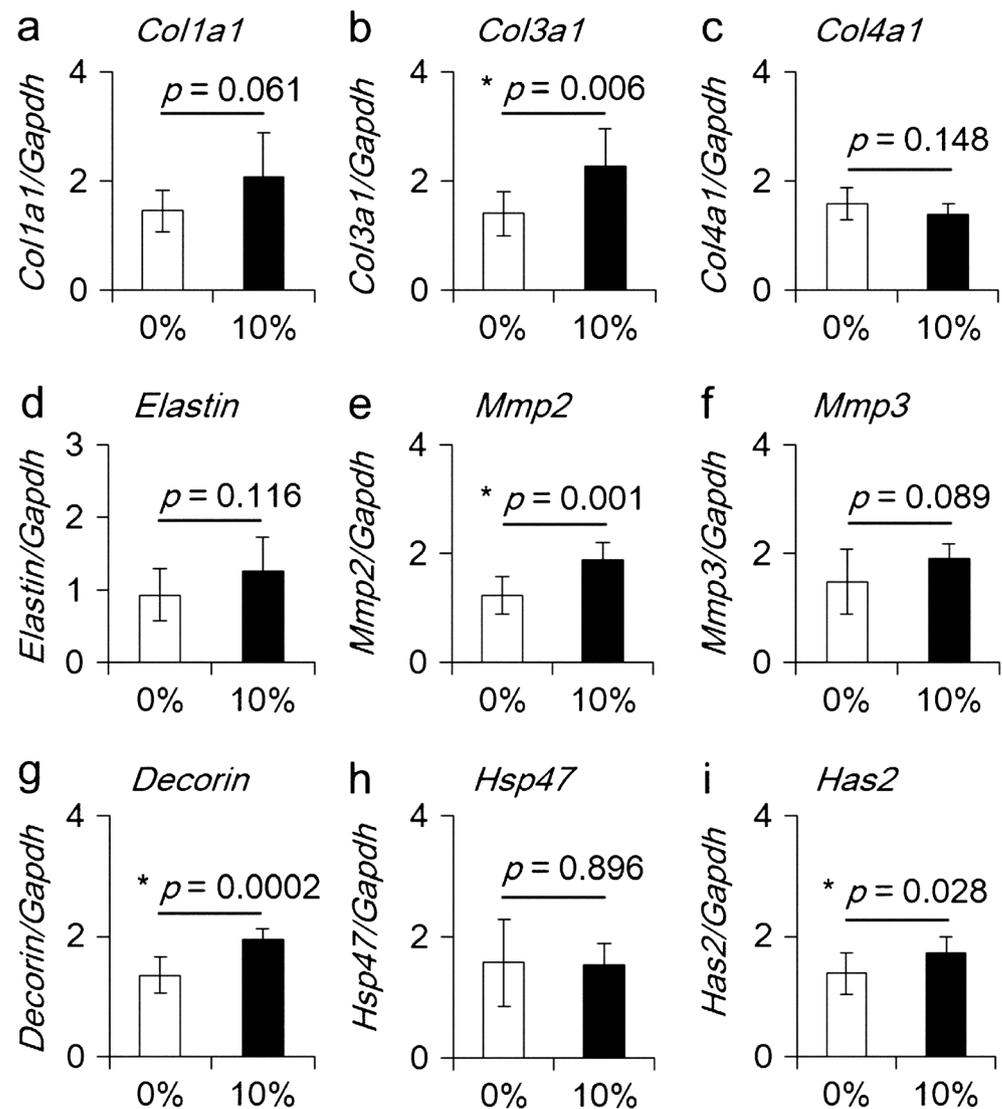

artificial phospholipid biomimetic interface (Ishihara and Takai 2009) containing the PMBN (2-methacryloyloxyethyl phosphorylcholine) polymer (Konno et al. 2004) on the surface of the tissue culture dishes and in a hairless mouse in vivo study as described above; therefore, we expected that an application of S-ESM on human skin may alter ECM gene expression in HDFs and skin elasticity. Accordingly, in this study, 1% S-ESM solution was applied to the arms of women for 12 weeks to evaluate skin elasticity after daily S-ESM application (Fig. 5). Skin elasticity was determined using skin biophysical techniques (Escoffier et al. 1989). Biological elasticity was increased significantly at all measurement regions of the arm compared with that before treatment. Additionally, net elasticity of the skin without viscous deformation was also significantly increased in the outer upper arm (Fig. 5e), outer forearm (Fig. 5g) and inner forearm regions (Fig. 5h) compared with that before application of 1% S-ESM lotion. In contrast, elasticity parameters of the skin were not affected

at the control site (Fig. 5a–d) where the control lotion (0% S-ESM) was applied before and after application.

Topical application of S-ESM improved facial wrinkles

As described above, skin wrinkles (Vierkotter et al. 2015) and elasticity (Çildağ and Çildağ 2017) are also correlated with lung fibrosis. In view of skin geroscience, to obtain additional information about the rejuvenation of mechanical properties of the extracellular matrix by S-ESM, a total of 21 women were recruited. Typical wrinkle replica binarization images showed that the wrinkle area decreased after S-ESM treatment (Fig. 6a–c) but not control treatment without eggshell membrane (Fig. 6d–f). Additionally, as shown in (Fig. 6g), the wrinkle area ratio in replica image analysis decreased after S-ESM lotion treatment. The wrinkle area ratio decreased significantly in the S-ESM group from 23.11% ± 1.41% before
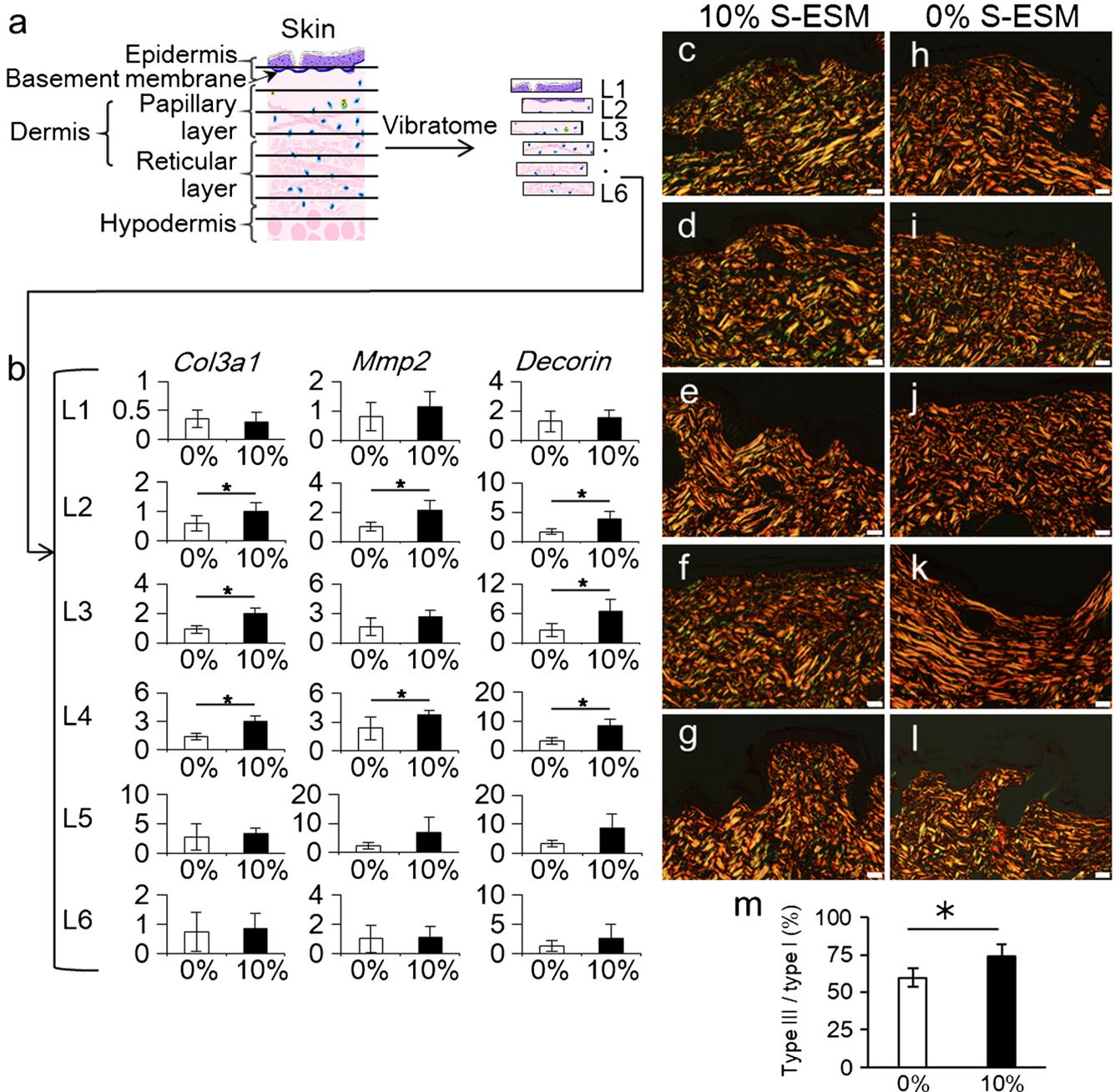
Fig. 4 S-ESM application increased type III collagen in the papillary dermis. **a** Skin structure and image of the skin layer separated by the vibratome. **b** Expression of *Col3*, *Mmp2* and *Decorin* expression in each layer after application of 0% or 10% S-ESM to the back skin of hairless mice for 10 days ($n = 6$). *$p < 0.05$. **c–l** Type III collagen was increased in the skin of hairless mice after S-ESM treatment for 10 days. Sections of mouse skin after application of 10% or 0% S-ESM were stained with Picrosirius Red. Green: type III collagen, red: type I collagen. Bar = 20 μm. **m** Green area (type III collagen)/red area (type I collagen) was calculated. Means ± SDs are shown ($n = 4$). *$p < 0.05$

application to 18.54% ± 1.76% after 1 week and 17.55% ± 1.21% after 2 weeks ($p = 0.027$ before application and 1 week after application; $p = 0.0003$ before application and 2 weeks after applications). In contrast, the ratio did not change significantly for the control group (22.13% ± 1.94% before application; 21.63% ± 1.60% after 1 week; 21.35% ± 1.40% after 2 weeks). These results showed that S-ESM had significant effects on wrinkle improvement.
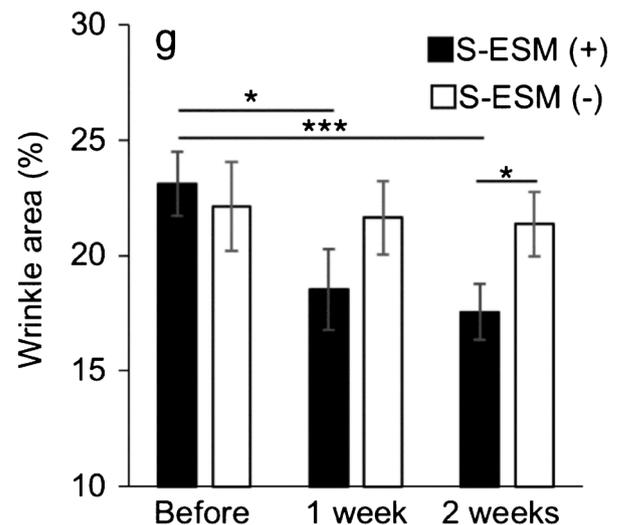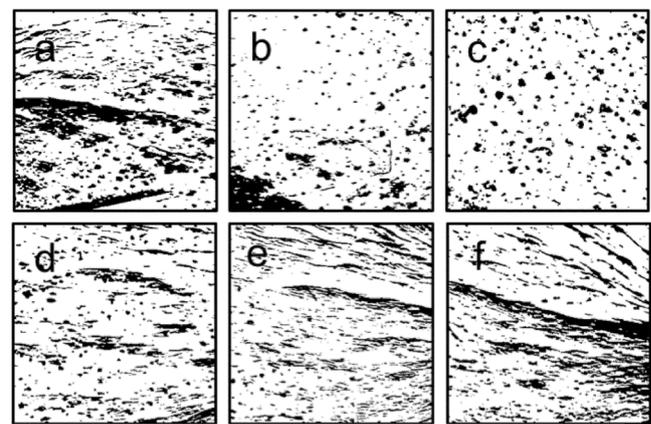
Discussion

Type III collagen is a type of fibrillar collagen and a homotrimer of three α1(III) chains. In the skin, papillary dermis is rich in type III collagen. However, the function of type III collagen in the skin has not yet been fully elucidated. In this study, we first focused on type III collagen and showed that a gel with a ratio of 20% type III collagen/80% type I collagen,
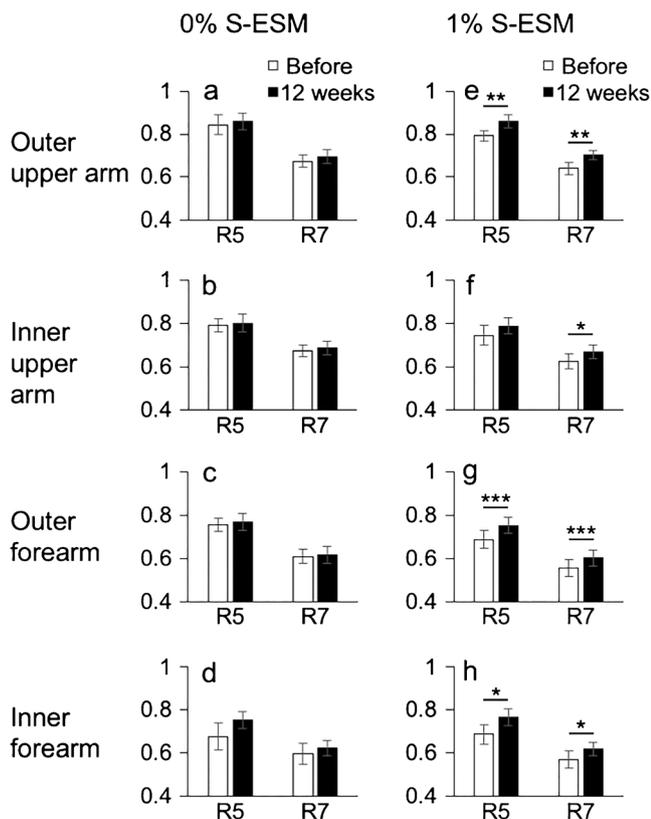
Fig. 5 Increased elasticity of human arm skin after application of S-ESM (**a**–**h**). Zero percent (**a**–**d**) or 1% S-ESM (**e**–**h**) solution was applied to the arm skin of women for 12 weeks and elasticity before and after the application was compared. Means ± SEs are shown ($n = 7$ per group). $*p < 0.05$, $**p < 0.01$, $***p < 0.001$ (paired sample t tests, two-tailed tests)

Fig. 6 S-ESM solution significantly reduced wrinkles in the outer corner of the eye in 1 week. **a**–**f** The replicas of the outer corner of the eye were collected before (**a**, **d**) and after 1 (**b**, **e**) or 2 (**c**, **f**) weeks of application of S-ESM (plus sign) (**b**, **c**) or S-ESM (minus sign) (**e**, **f**) solution. The images were obtained by applying light from a certain direction to the replica of the outer corner of the eye. **g** The wrinkle area ratio analyzed from the replica is shown. Means ± SEs are given ($n = 21$ per group). $*p < 0.05$, $***p < 0.001$ (paired sample t tests, two-tailed tests)

similar to that of the baby skin, resulted in higher elasticity and higher gene expression of type III collagen and a higher HDF mitochondrial activity than that with 100% type I collagen ($p < 0.05$; Fig. 1). Furthermore, ESM application to mice skin showed that the expression of genes encoding type III collagen, decorin and MMP2 was increased and the levels of type III collagen were also elevated (Fig. 3), as demonstrated by Picrosirius red staining–polarization microscopy that distinguishes collagen fiber type in S-ESM-treated pupillary skin (Fig. 4; Fig. S2 and Fig. S3) through biochemical and histochemical analyses after application of ESM. Moreover, ESM application improved human skin elasticity (Fig. 5). Thus, increased type III collagen induced by S-ESM application in the skin was related to increased skin elasticity.

Type III collagen fibers are thinner than type I collagen fibers and have a flexible structure (Flexi-rod structure) (Parkin et al. 2017). The primary function of type III collagen is fibril formation of type I collagen (Liu et al. 1997). As a component of the ECM, type III collagen is essential not only for the developing skin and cardiovascular system but also to maintain internal organs and adult skin (Olsen 1995). Type III collagen is associated with skin elasticity and patients with deletion of type III collagen exhibit loss of skin elasticity

and blood vessel formation, resulting in Ehlers–Danlos syndrome (Kontusaari et al. 1990; Kuivaniemi et al. 1995; Prockop and Kivirikko 1984). Type III collagen is present at higher levels in the papillary dermis (just below the basal membrane) than in the reticular dermis (Meigel et al. 1977; Ramshaw 1986; Weber et al. 1984). Additionally, decorin, which regulates the assembly of collagen fibrils, is also abundant in the papillary dermis (Reed and Iozzo 2002; Schonherr et al. 1993). However, age-related changes in type III collagen and decorin in the skin affect the physical properties of the skin (Carrino et al. 2000, 2003; Ramshaw 1986). Notably, in this study, we found that gels with type III collagen to type I collagen ratios of 20:80 had the highest elasticity and HDF mitochondrial activity. Additionally, HDFs on the gel changed to a spherical form (similar to stem cells) from a spindle-shaped form (similar to fibroblasts) (Fig. S4). This ratio

(III:I = 20:80) was similar to that observed in the baby skin (Smith et al. 1986). Although the detailed molecular mechanisms have not yet been clarified, an ECM environment with moderate elasticity seems to be suitable for cells and ESM can induce a healthy state in the skin, improving the functions of dermal and epidermal cells.

ESM application also induced decorin and MMP2 in the papillary layer in this study in addition to type III collagen. The papillary dermis just below the basal membrane contains skin stem cells (Li et al. 2010) and capillaries develop to supply nutrients to dermal fibroblasts and epidermal basal cells in this region (Yen and Braverman 1976). Stem cells are maintained in elastic and soft tissues (Winer et al. 2009) and tissue stiffness resulting from prolonged ECM changes results in progression of the diseased state (Handorf et al. 2015). The function of decorin was not analyzed in this study. Gel analyses using decorin and other ECM molecules in type I collagen may be useful to elucidate the different mechanisms between papillary and reticular dermis in terms of their material quality. Proteoglycans, elastin and hyaluronic acid in the skin are viscoelastic molecules. Elastin forms elastic fibers in the skin and decreases with age (Pasquali-Ronchetti and Baccarani-Contri 1997; Uitto 2008). Elastic fibers increase from the papillary dermis to the reticular dermis (Vitellaro-Zuccarello et al. 1994). Our results did not reveal the effects of ESM on elastin expression. Therefore, the effects of ESM seemed to be specific to the papillary dermis and to modulate the ECM environment of the papillary layer, similar to that in the young state.

Dryness, roughness and wrinkles characterize physiologically aged skin. With aging, dermal collagen synthesis and cell populations decrease and MMP levels increase (Chung et al. 2001; Varani et al. 2000). Additionally, dermal thickness decreases as dermal collagen content is reduced (Castelo-Branco et al. 1994; Kurban and Bhawan 1990). The ECM, which contains collagen fibers, elastin, proteoglycans, glycosaminoglycans and adhesion molecules and makes up the dermis, functions to maintain mechanical tension and elasticity and is involved in tissue support and crosslinking and as a physical border. Therefore, loss of ECM components decreases skin elasticity (Berardesca et al. 1991; Nishimori et al. 2001; Ventre et al. 2009). Interestingly, poor trunk flexibility (one of the components of physical fitness) is associated with arterial stiffening (Yamamoto et al. 2009).

In summary, in this study, we found that ESM had antiaging effects by improving the ECM environment in the papillary layer. ESM is available worldwide and is a biomaterial with application in medical, food and cosmetic fields. Thus, natural products, such as ESM, from traditional Asian medicine may provide new approaches to improving health.

Compliance with ethical standards

Animal experiments were conducted with the ethical approval of the University of Tokyo Animal Experiments Committee and Tokyo University of Agriculture and Technology Animal Experiments Committee. Approval for this study was obtained from the Ethics Committee of the University of Tokyo.

References

Aiba-Kojima E, Tsuno NH, Inoue K, Matsumoto D, Shigeura T, Sato T, Suga H, Kato H, Nagase T, Gonda K, Koshima I, Takahashi K, Yoshimura K (2007) Characterization of wound drainage fluids as a source of soluble factors associated with wound healing: comparison with platelet-rich plasma and potential use in cell culture. Wound Repair Regen 15:511–520

Archid R, Patzelt A, Lange-Asschenfeldt B, Ahmad SS, Ulrich M, Stockfleth E, Philipp S, Sterry W, Lademann J (2012) Confocal laser-scanning microscopy of capillaries in normal and psoriatic skin. J Biomed Opt 17:101511

Arias JL, Fernandez MS, Dennis JE, Caplan AI (1991) Collagens of the chicken eggshell membranes. Connect Tissue Res 26:37–45

Arias JL, Carrino DA, Fernandez MS, Rodriguez JP, Dennis JE, Caplan AI (1992) Partial biochemical and immunochemical characterization of avian eggshell extracellular matrices. Arch Biochem Biophys 298:293–302

Auer T, Bacharach-Buhles M, el-Gammal S, Stucker M, Panz B, Popp C, Hoffmann K, Happe M, Altmeyer P (1994) The hyperperfusion of the psoriatic plaque correlates histologically with dilatation of vessels. Acta Derm Venereol Suppl (Stockh) 186:30–32

Berardesca E, Farinelli N, Rabbiosi G, Maibach HI (1991) Skin bioengineering in the noninvasive assessment of cutaneous aging. Dermatologica 182:1–6

Braverman IM (1983) The role of blood vessels and lymphatics in cutaneous inflammatory processes: an overview. Br J Dermatol 109(Suppl 25):89–98

Carrino DA, Sorrell JM, Caplan AI (2000) Age-related changes in the proteoglycans of human skin. Arch Biochem Biophys 373:91–101

Carrino DA, Onnerfjord P, Sandy JD, Cs-Szabo G, Scott PG, Sorrell JM, Heinegard D, Caplan AI (2003) Age-related changes in the proteoglycans of human skin. Specific cleavage of decorin to yield a major catabolic fragment in adult skin. J Biol Chem 278:17566–17572

Castelo-Branco C, Pons F, Gratacos E, Fortuny A, Vanrell JA, Gonzalez-Merlo J (1994) Relationship between skin collagen and bone changes during aging. Maturitas 18:199–206

Chung JH, Seo JY, Choi HR, Lee MK, Youn CS, Rhie G, Cho KH, Kim KH, Park KC, Eun HC (2001) Modulation of skin collagen metabolism in aged and photoaged human skin in vivo. J Invest Dermatol 117:1218–1224

Çildağ S, Çildağ M (2017) The relationship between the degree of skin fibrosis by sonoelastography and the degree of pulmonary involvement in scleroderma. Turk J Med Sci 47:1702–1744

Cossarizza A, Kalashnikova G, Grassilli E, Chiappelli F, Salvioli S, Capri M, Barbieri D, Troiano L, Monti D, Franceschi C (1994) Mitochondrial modifications during rat thymocyte apoptosis: a study at the single cell level. Exp Cell Res 214:323–330

D'Hondt S, Guillemyn B, Syx D, Symoens S, De Rycke R, Vanhoutte L, Toussaint W, Lambrecht BN, De Paepe A, Keene DR, Ishikawa Y, Bachinger HP, Janssens S, Bertrand MJM, Malfait F (2018) Type III collagen affects dermal and vascular collagen fibrillogenesis and tissue integrity in a mutant Col3a1 transgenic mouse model. Matrix Biol 70:72–83

Dorrie J, Gerauer H, Wachter Y, Zunino SJ (2001) Resveratrol induces extensive apoptosis by depolarizing mitochondrial membranes and activating caspase-9 in acute lymphoblastic leukemia cells. Cancer Res 61:4731–4739

Du J, Hincke MT, Rose-Martel M, Hennequet-Antier C, Brionne A, Cogburn LA, Nys Y, Gautron J (2015) Identifying specific proteins involved in eggshell membrane formation using gene expression analysis and bioinformatics. BMC Genomics 16:792

Escoffier C, de Rigal J, Rochefort A, Vasselet R, Leveque JL, Agache PG (1989) Age-related mechanical properties of human skin: an in vivo study. J Invest Dermatol 93:353–357

Exposito JY, Valcourt U, Cluzel C, Lethias C (2010) The fibrillar collagen family. Int J Mol Sci 11:407–426

Gilhar A, Ullmann Y, Karry R, Shalaginov R, Assy B, Serafimovich S, Kalish RS (2004) Aging of human epidermis: reversal of aging changes correlates with reversal of keratinocyte fas expression and apoptosis. J Gerontol A Biol Sci Med Sci 59:411–415

Gunn DA, de Craen AJ, Dick JL, Tomlin CC, van Heemst D, Catt SD, Griffiths T, Ogden S, Maier AB, Murray PG, Griffiths CE, Slagboom PE, Westendorp RG (2013) Facial appearance reflects human familial longevity and cardiovascular disease risk in healthy individuals. J Gerontol A Biol Sci Med Sci 68:145–152

Ha YW, Son MJ, Yun KS, Kim YS (2007) Relationship between eggshell strength and keratan sulfate of eggshell membranes. Comp Biochem Physiol A Mol Integr Physiol 147:1109–1115

Handorf AM, Zhou Y, Halanski MA, Li WJ (2015) Tissue stiffness dictates development, homeostasis, and disease progression. Organogenesis 11:1–15

Ishihara K, Takai M (2009) Bioinspired interface for nanobiodevices based on phospholipid polymer chemistry. J R Soc Interface 6(Suppl 3):S279–S291

Konno T, Watanabe J, Ishihara K (2004) Conjugation of enzymes on polymer nanoparticles covered with phosphorylcholine groups. Biomacromolecules 5:342–347

Konttinen YT, Mackiewicz Z, Ruuttila P, Ceponis A, Sukura A, Povilenaite D, Hukkanen M, Virtanen I (2003) Vascular damage and lack of angiogenesis in systemic sclerosis skin. Clin Rheumatol 22:196–202

Kontusaari S, Tromp G, Kuivaniemi H, Romanic AM, Prockop DJ (1990) A mutation in the gene for type III procollagen (COL3A1) in a family with aortic aneurysms. J Clin Invest 86:1465–1473

Krueger N, Luebberding S, Oltmer M, Streker M, Kerscher M (2011) Age-related changes in skin mechanical properties: a quantitative evaluation of 120 female subjects. Skin Res Technol 17:141–148

Kuivaniemi H, Tromp G, Bergfeld WF, Kay M, Helm TN (1995) Ehlers-Danlos syndrome type IV: a single base substitution of the last nucleotide of exon 34 in COL3A1 leads to exon skipping. J Invest Dermatol 105:352–356

Kurban RS, Bhawan J (1990) Histologic changes in skin associated with aging. J Dermatol Surg Oncol 16:908–914

Li L, Fukunaga-Kalabis M, Yu H, Xu X, Kong J, Lee JT, Herlyn M (2010) Human dermal stem cells differentiate into functional epidermal melanocytes. J Cell Sci 123:853–860

Liu X, Wu H, Byrne M, Krane S, Jaenisch R (1997) Type III collagen is crucial for collagen I fibrillogenesis and for normal cardiovascular development. Proc Natl Acad Sci U S A 94:1852–1856

Liu Z, Zhang F, Li L, Li G, He W, Linhardt RJ (2014) Compositional analysis and structural elucidation of glycosaminoglycans in chicken eggs. Glycoconj J 31:593–602

Meigel WN, Gay S, Weber L (1977) Dermal architecture and collagen type distribution. Arch Dermatol Res 259:1–10

Nishimori Y, Edwards C, Pearse A, Matsumoto K, Kawai M, Marks R (2001) Degenerative alterations of dermal collagen fiber bundles in photodamaged human skin and UV-irradiated hairless mouse skin: possible effect on decreasing skin mechanical properties and appearance of wrinkles. J Invest Dermatol 117:1458–1463

Ohto-Fujita E, Konno T, Shimizu M, Ishihara K, Sugitate T, Miyake J, Yoshimura K, Taniwaki K, Sakurai T, Hasebe Y, Atomi Y (2011) Hydrolyzed eggshell membrane immobilized on phosphorylcholine polymer supplies extracellular matrix environment for human dermal fibroblasts. Cell Tissue Res 345:177–190

Olsen BR (1995) The roles of collagen genes in skeletal development and morphogenesis. Experientia 51:194–195

Parkin JD, San Antonio JD, Persikov AV, Dagher H, Dalgleish R, Jensen ST, Jeunemaitre X, Savige J (2017) The collalphagen III fibril has a "flexi-rod" structure of flexible sequences interspersed with rigid bioactive domains including two with hemostatic roles. PLoS One 12:e0175582

Pasquali-Ronchetti I, Baccarani-Contri M (1997) Elastic fiber during development and aging. Microsc Res Tech 38:428–435

Prockop DJ, Kivirikko KI (1984) Heritable diseases of collagen. N Engl J Med 311:376–386

Ramshaw JA (1986) Distribution of type III collagen in bovine skin of various ages. Connect Tissue Res 14:307–314

Reed CC, Iozzo RV (2002) The role of decorin in collagen fibrillogenesis and skin homeostasis. Glycoconj J 19:249–255

Roshdy HS, Soliman MH, El D II, Ghonemy S (2018) Skin aging parameters: a window to heart block. Clin Cardiol 41:51–56

Sauermann K, Gambichler T, Jaspers S, Radenhausen M, Rapp S, Reich S, Altmeyer P, Clemann S, Teichmann S, Ennen J, Hoffmann K (2002) Histometric data obtained by in vivo confocal laser scanning microscopy in patients with systemic sclerosis. BMC Dermatol 2:8

Schonherr E, Beavan LA, Hausser H, Kresse H, Culp LA (1993) Differences in decorin expression by papillary and reticular fibroblasts in vivo and in vitro. Biochem J 290(Pt 3):893–899

Smith LT, Holbrook KA, Madri JA (1986) Collagen types I, III, and V in human embryonic and fetal skin. Am J Anat 175:507–521

Task Force Committee for Evaluation of Anti-Aging Function (2007) Guidelines for evaluation of anti-wrinkle products. J Jpn Cosmet Sci Soc 31:411–431

Uitto J (2008) The role of elastin and collagen in cutaneous aging: intrinsic aging versus photoexposure. J Drugs Dermatol 7:s12–s16

Varani J, Warner RL, Gharaee-Kermani M, Phan SH, Kang S, Chung JH, Wang ZQ, Datta SC, Fisher GJ, Voorhees JJ (2000) Vitamin A antagonizes decreased cell growth and elevated collagen-degrading matrix metalloproteinases and stimulates collagen accumulation in naturally aged human skin. J Invest Dermatol 114:480–486

Ventre M, Mollica F, Netti PA (2009) The effect of composition and microstructure on the viscoelastic properties of dermis. J Biomech 42:430–435

Vierkotter A, Schikowski T, Sugiri D, Matsui MS, Kramer U, Krutmann J (2015) MMP-1 and -3 promoter variants are indicative of a common

susceptibility for skin and lung aging: results from a cohort of elderly women (SALIA). J Invest Dermatol 135:1268–1274

Vitellaro-Zuccarello L, Cappelletti S, Dal Pozzo Rossi V, Sari-Gorla M (1994) Stereological analysis of collagen and elastic fibers in the normal human dermis: variability with age, sex, and body region. Anat Rec 238:153–162

Vybohova D, Mellova Y, Adamicova K, Adamkov M, Heskova G (2012) Quantitative changes of the capillary bed in aging human skin. Histol Histopathol 27:961–967

Wang W (2005) Oxygen partial pressure in outer layers of skin: simulation using three-dimensional multilayered models. Microcirculation 12:195–207

Wang W, Winlove CP, Michel CC (2003) Oxygen partial pressure in outer layers of skin of human finger nail folds. J Physiol 549:855–863

Weber L, Kirsch E, Muller P, Krieg T (1984) Collagen type distribution and macromolecular organization of connective tissue in different layers of human skin. J Invest Dermatol 82:156–160

Winer JP, Janmey PA, McCormick ME, Funaki M (2009) Bone marrow-derived human mesenchymal stem cells become quiescent on soft substrates but remain responsive to chemical or mechanical stimuli. Tissue Eng A 15:147–154

Wong M, Hendrix MJ, von der Mark K, Little C, Stern R (1984) Collagen in the egg shell membranes of the hen. Dev Biol 104:28–36

Yamamoto K, Kawano H, Gando Y, Iemitsu M, Murakami H, Sanada K, Tanimoto M, Ohmori Y, Higuchi M, Tabata I, Miyachi M (2009) Poor trunk flexibility is associated with arterial stiffening. Am J Physiol Heart Circ Physiol 297:H1314–H1318

Yamato M, Yamamoto K, Hayashi T (1992) Decrease in cellular potential of collagen gel contraction due to in vitro cellular aging: a new aging index of fibroblast with high sensitivity. Connective Tissue 24:157–162

Yen A, Braverman IM (1976) Ultrastructure of the human dermal microcirculation: the horizontal plexus of the papillary dermis. J Invest Dermatol 66:131–142